Comparative Molecular Field Analysis Study of Stilbene Derivatives Active against A549 Lung Carcinoma

Sanghee KIM,[a] Sun Young MIN,[b] Sang Kook LEE,[c] and Won-Jea CHO*,[b]

[a] *Natural Products Research Institute, College of Pharmacy, Seoul National University; Seoul 110–460, Korea:* [b] *College of Pharmacy, Chonnam National University; Yongbong-dong Buk-gu, Kwangju 500–757, Korea: and* [c] *College of Pharmacy, Ewha Womans University; Seoul 120–750, Korea.* Received December 9, 2002; accepted February 13, 2003

A series of 43 stilbene derivatives that showed cytotoxicity against human lung carcinoma (A549) was analyzed using comparative molecular field analysis (CoMFA) for defining the hypothetic pharmacophore model. The polyoxylated stilbenes were found to be active inhibitors of tubulin polymerization. Several *cis*-stilbenes are structurally similar to combretastatins. However, the *trans*-stilbenes are assumed to be close to resveratrol found in grapes and have been reported to be potential cancer chemopreventive agents by modulating the initiation, promotion, and progression of the carcinogenic process. With several synthesized compounds that were evaluated for antitumor cytotoxicity against human lung tumor cells (A549), the stilbene derivatives were subjected to CoMFA. To perform systematic molecular modeling of these compounds, a conformational search was carried out based on the precise dihedral angle analysis of the lead compound (1p). The X-ray crystallographic structure of combretastatin A-1 was also used for defining the active conformers of the compounds. After determining the energy-minimized conformers of the lead compound (1p), CoMFA was performed using five different alignments. The three dimensional (3D)-quantitative structure–activity relationship study resulted in reasonable cross-validated, conventional r^2 values equal to 0.640 and 0.958, respectively.

Key words stilbene; cytotoxicity; A-549; comparative molecular field analysis (CoMFA); combretastatin

Many efforts for the development of chemopreventive or therapeutic agents for cancer from natural products have been performed over the last several decades. As potential antitumor agents, polymethoxy stilbenes and dihydrostilbenes have been investigated.[1,2] Combretastatins, a branch of stilbene derivatives, have been isolated from the South African tree *Combretum*.[3,4] Among these combretastatins, combretastatin A-4 was found to exhibit the most potent cytotoxicity. These compounds are known to inhibit tubulin polymerization, to cause mitotic arrest in L1210 murine leukemia cells, and competitively inhibit the binding of radio-labeled colchicines to tubulin.[5] Moreover, a recent study of combretastatins verified that combretastatin A-4 exhibits potent activity against multidrug-resistant (MDR) cancer cells.[6] This compound has been evaluated for clinical application, resulting in only limited success due to its poor water solubility.[7] Recently, the more water-soluble phosphate derivatives of combretastatin A-4 have undergone clinical evaluation. From these efforts, the development of new stilbene analogues continues to attract interest as a way to obtain potential antitumor therapeutic targets (Chart 1).

Several molecular modeling studies involving stilbenes used as antitumor agents have been reported. The proposed models predicted the activity of combretastatin binding to the colchicine binding site, but the models showed limited success and usefulness.[8—10] Two-dimensional (2D) models related to stilbene derivatives that showed tubulin polymerization inhibitory activity were also studied. However, the lack of structural variation and an inability to predict activity are the limitations of the models.

As part of our research on stilbenes exhibiting selective human cytochrome P450 1B1 inhibition,[11] we evaluated the cytotoxicity of the prepared compounds against several tumor cell lines. A comparative molecular field analysis (CoMFA), ligand-based drug design tool, one of the most commonly used three dimensional quantitative structure–activity relationship (3D-QSAR) programs, has also been applied to a number of different classes of compounds.[12,13] A CoMFA study of the stilbenes that showed cytotoxicity against A549 lung carcinoma was performed to yield a relatively high cross-validated r^2 value. In the present study, the model is constructed using various substituents of aromatic rings of stilbenes and diverse hetoroaromatic rings because it is well known that a 3D-QSAR study of diversely modified molecules showing a wide range of activity results in a reliable pharmacophore model (Chart 2).

Experimental

Biological Data Table 1 lists the structures and the observed and calculated biological activity values of compounds forming the training set used to derive the CoMFA model. In this study, biological activity refers only to the cytotoxicity value expressed as pIC_{50}, that is, the $-\log$ of the concentration (M) of the tested compounds that inhibited tumor cell growth by 50%. Consequently, all the activity values are in the range of 4.46 (lowest active compound) to 7.54 (most active compound). The cytotoxicity (the IC_{50} value) of compounds **1b**, **1j**—**m**, and **2i**—**l** were obtained by the sulforhodamine B (SRB) method.[14,15] Except for the above-mentioned compounds, the MTT colorimetric assay method was employed.[16,17] In general, tabulating biological activity data from different sources should be done very carefully. For this work we have selected diverse compounds of which the activity was measured by two different methods. Because the MTT and SRB methods yielded similar results,[18] we felt confident that all the data are compatible with each other. Experimental procedures of the SRB method were followed up with the US National Cancer Institute protocol as follows. Briefly, tumor cells were cultured to maintain logarithmic growth by changing the medium 24 h before cytotoxicity assays. On the day of the assay, the cells were harvested by trypsinization, counted, diluted in media, and added to 96-well plates. The number of tumor cells (A549) used was 1×10^4/well. The cells were then preincubated for 24 h in a 5% CO_2 incubator at 37 °C. The compounds dissolved in dimethyl sulfoxide (DMSO) were added to the wells in six 2-fold dilutions starting from the highest concentrations, and incubated for 48 h in a 5% CO_2 incubator at 37 °C. The final DMSO concentration was 0.05%. At the termination of the incubation, the culture medium in each well was removed, and the cells were fixed with cold 10% trichloroacetic acid (TCA) for 1 h at room temperature. The microplates were washed, dried, and stained with 0.4% SRB in 1% acetic acid for 30 min at room temperature. The cells were washed again and the bound stain was

* To whom correspondence should be addressed. e-mail: wjcho@chonnam.ac.kr

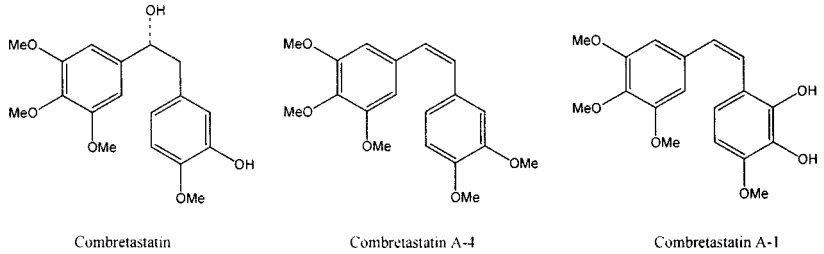

Chart 1. The Structure of Combretastatin A4 and A1

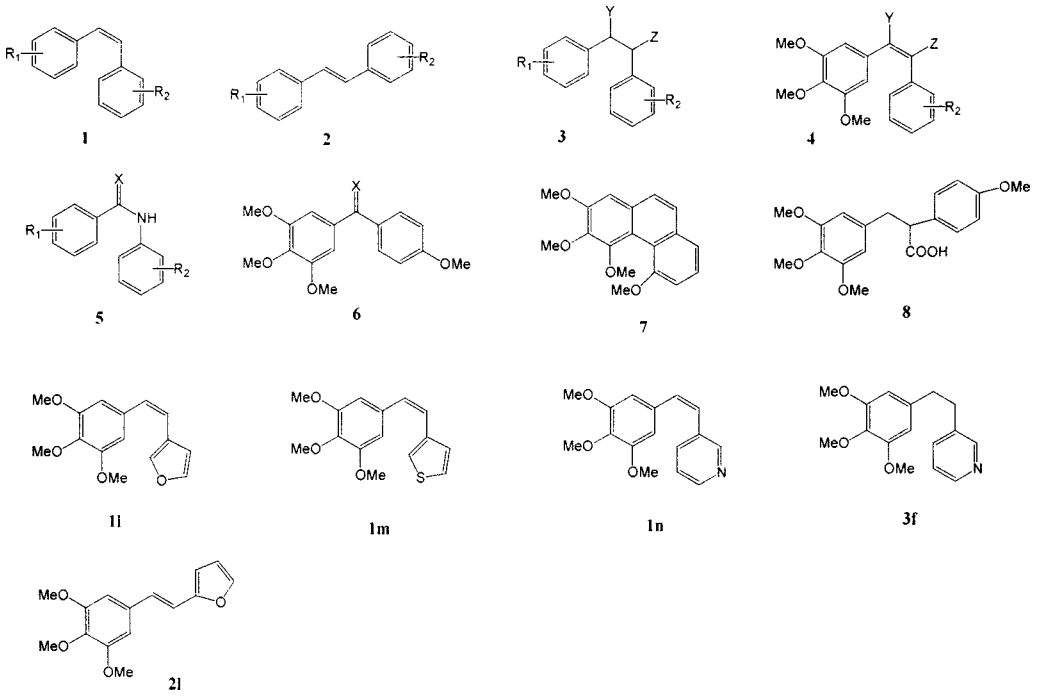

Chart 2. The Structure of Combretastatin Derivatives

solubilized with 10 mM Tris base solution (pH 10.5), and the absorbances were measured spectrophotometrically at 520 nm on a microtiter plate reader (Molecular Devices, Sunnyvale, CA, U.S.A.). The data were transformed into Lotus-123 format and survival fractions were calculated by regression analysis (plotting the cell viability versus the concentration of the test compound). The IC_{50} values represent the concentrations of the compounds that inhibit 50% of cell growth. All data represent the mean values for a minimum of three wells.

Computer Modeling The computational calculations were performed using the molecular modeling software Sybyl 6.30 on an Indigo2 workstation (Silicon Graphics) with the standard bond lengths and angles.[19] Molecular mechanics calculations including field-fit optimization were carried out with the standard Tripos force field and the minimum energy change of 0.05 kcal/mol as a convergence criteria. Charges were calculated using the Gasteiger-Huckel method as implemented in Sybyl. To find candidates for local minimum conformation, a preliminary conformational search was performed by the systematic search method and grid search implemented in the Sybyl system. Conformational search of **1p** was performed in 30-degree increments in two sigma bonds (τ1, τ2) and 20 conformers were selected as shown in Table 2. For defining the active conformer of **1p**, each conformer employed energy minimization again by the Tripos force field method. As a result, conformers 1, 11, 14, and 16 gave the same conformation (τ1; 41.6°, τ2; 47.3°) with the same energy (16.845 kcal). Four conformers could also be derived by the above analysis. Finally, we selected conformers 1—3, 8, and 12 as the representatives for CoMFA study. The lowest-energy minimum conformation of each compound was assumed to be the active conformer. However, it was difficult to determine the active conformers among these conformers because the value of the energy difference is too small to exclude the lower values. Therefore we employed CoMFA using each conformer as a template molecule to obtain the results depicted in Table 3. The proposed active conformer of **1p** was arbitrarily selected as a template molecule and the other compounds were superposed on it by matching the corresponding atoms of the stilbene derivatives of each molecule due to similar rigidity. The grid in which the molecules were regularly spaced (2 Å) with 19×22×22 Å (X=−14 to 5, Y=−10 to 12, Z=−12 to 10) dimensions was determined by an automatic procedure performed by the Sybyl-CoMFA module. When the region for the molecules to be embedded in the grid box with dimensions of 16×18×14 Å (X=−11 to 5, Y=−7 to 11, Z=−10 to 4) was manually defined, lower statistical values such as q^2 and r^2 were obtained. As the initial conformations of the compounds, the X-ray crystallographic data obtained from the Cambridge Crystallographic Data Center (CCDC) of combretastatin A-1 were also utilized.[20] We used it as a template molecule for determining the conformation of the molecules. To investigate the conformation profile, we carried out an extensive conformational search of the compounds using the torsion angle of combretastatin A-1. The torsion angles of τ1 (−58.1°) and τ2 (−15.7°) in the compound were fixed and each active conformer of the 43 compounds was superimposed on that of the template molecule, so that each structural component was as close as possible to the corresponding components of the reference. Thus, eight atoms, *i.e.*, A-ring and C2—C3 atoms were selected because most of the compounds consist of these atoms as a common unit, and the sum of the squares of the distance of the eight atomic positions from the corresponding atomic positions of the reference compound was made as small as possible for the superimposition, as shown in Chart 3. However, this procedure gave less reliable statistical values of q^2 as well as r^2, as shown in Table 4. For performing CoMFA, steric and electrostatic interaction energies were calculated using a carbon sp^3 probe atom with a charge of +1, and an energy cutoff of 30 kcal/mol. Using the Sybyl implementation of the partial least-squares

Table 1. Observed and Calculated Cytotoxicity Values against A549 Carcinoma of the Compounds and cLog P

No.	Compd.	R1	R2	X	Y	Z	pIC_{50}[d]			cLog P[e]
							Obsd.	Calcd.	Diff.	
1	**1a**[b]	3,4,5-$(OMe)_3$	4-OPr^n	—	—	—	7.40	7.41	−0.01	4.30
2	**1b**[c]	3,4,5-$(OMe)_3$	4-Br	—	—	—	7.54	7.27	0.27	4.19
3	**1c**[a]	3,4,5-$(OMe)_3$	3-OMe	—	—	—	6.89	6.68	0.21	3.25
4	**1d**[a]	3,4,5-$(OMe)_3$	2-OMe	—	—	—	5.96	6.33	−0.37	3.25
5	**1e**[a]	3,4,5-$(OMe)_3$	4-OMe	—	—	—	6.01	5.95	0.06	3.25
6	**1f**[b]	3,4,5-$(OMe)_3$	2-Cl 4-OMe	—	—	—	7.29	7.37	−0.08	4.10
7	**1g**[a]	3,4,5-$(OMe)_3$	H	—	—	—	6.77	6.57	0.20	3.33
8	**1h**[a]	3,4,5-$(OMe)_3$	4-Cl	—	—	—	7.10	7.14	−0.04	4.04
9	**1i**[a]	3,4,5-$(OMe)_3$	4-OAc	—	—	—	5.77	5.78	−0.01	2.68
10	**1j**[c]	3,5-$(OMe)_2$	4-OMe	—	—	—	6.62	6.65	−0.03	4.36
11	**1k**[c]	3,5-$(OMe)_2$	2,4,5-$(OMe)_3$	—	—	—	5.35	5.43	−0.08	3.89
12	**1l**[c]	1-(3-furanyl)-2-(3,4,5-trimethoxyphenyl)ethene					6.12	5.76	0.36	2.50
13	**1m**[c]	1-(3-thiophenyl)-2-(3,4,5-trimethoxyphenyl)ethene					5.12	5.56	−0.44	2.97
14	**1n**[a]	1-(4-pyridyl)-2-(3,4,5-trimethoxyphenyl)ethene					4.85	4.91	−0.06	1.83
15	**1o**[a]	1-(3-pyridyl)-2-(3,4,5-trimethoxyphenyl)ethene					4.86	4.99	−0.13	1.83
16	**2a**[b]	3,4,5-$(OMe)_3$	4-OEt	—	—	—	6.77	6.57	0.20	3.78
17	**2c**[b]	3,4,5-$(OMe)_3$	4-SMe	—	—	—	6.33	6.23	0.10	3.89
18	**2d**[b]	3,4,5-$(OMe)_3$	4-Me	—	—	—	5.96	6.24	−0.28	3.83
19	**2e**[b]	3,4,5-$(OMe)_3$	4-Et	—	—	—	6.89	6.70	0.19	4.36
20	**2f**[c]	3,4,5-$(OMe)_3$	4-OMe	—	—	—	6.88	6.64	0.24	3.25
21	**2g**[a]	3,4,5-$(OMe)_3$	4-OAc	—	—	—	5.01	5.04	−0.03	2.68
22	**2h**[a]	3,4,5-$(OMe)_3$	2,3,4-$(OMe)_3$	—	—	—	4.90	4.89	0.01	2.22
23	**2i**[c]	3,5-$(OMe)_2$	4-OMe	—	—	—	5.53	5.46	0.07	4.36
24	**2j**[c]	3,5-$(OMe)_2$	2,4-$(OMe)_2$	—	—	—	5.58	5.35	0.24	4.45
25	**2k**[c]	3,5-$(OMe)_2$	2-OH 4-OMe	—	—	—	6.62	6.41	0.21	3.87
26	**2l**[c]	1-(2-furanyl)-2-(3,4,5-trimethoxyphenyl)ethene				—	4.46	4.65	−0.19	2.50
27	**3a**[b]	3,4,5-$(OMe)_3$	4-OEt	—	H	H	6.72	6.75	−0.03	3.93
28	**3b**[b]	3,4,5-$(OMe)_3$	4-SMe	—	H	H	6.82	6.96	−0.14	4.04
29	**3c**[b]	3,4,5-$(OMe)_3$	4-Et	—	H	H	7.06	7.40	−0.34	4.51
30	**3d**[a]	3,4,5-$(OMe)_3$	4-NH_2	—	H	H	4.91	4.77	0.14	2.25
31	**3e**[b]	3,4,5-$(OMe)_3$	4-OMe	—	H	CN	4.94	4.96	−0.02	2.10
32	**3f**[a]	1-(3-pyridyl)-2-(3,4,5-trimethoxyphenyl)ethane					4.91	4.66	0.25	1.98
33	**4a**[b]	—	4-OMe	—	COOH	H	4.86	5.04	−0.18	2.25
34	**4b**[b]	—	4-OMe	—	H	COOH	5.28	5.24	0.04	2.25
35	**4c**[b]	—	3-OMe	—	COOMe	H	5.89	6.02	−0.03	2.63
36	**4d**[b]	—	4-OMe	—	CONHEt	H	5.47	5.58	−0.11	2.44
37	**4e**[b]	—	4-OMe	—	$COO(CH_2)_2NEt_2$	H	5.74	5.90	−0.16	3.65
38	**5a**[a]	3,4,5-$(OMe)_3$	4-OMe	O	—	—	4.85	4.99	−0.13	1.68
39	**5b**[a]	3,5-$(OMe)_2$	4-OMe	H_2	—	—	5.24	5.33	−0.09	3.20
40	**6a**[b]	—	—	H, OH	—	—	5.82	5.74	0.08	1.26
41	**6b**[b]	—	—	H_2	—	—	6.82	6.91	−0.09	3.02
42	**7**[b]	—	—	—	—		5.24	5.21	0.03	3.31
43	**8**[b]	—	—	—	—	—	4.84	4.79	0.05	1.95

a) Biological data taken from ref. 21, *b*) biological data taken from ref. 22, *c*) biological data were obtained by the SRB method and the synthesis was reported in ref. 11, *d*) −log molar concentration, *e*) calculated Log P value was obtained from the Sybyl 6.3 program.

(PLS) analysis, regression analyses were performed initially with the leave-one-out cross-validation method to reduce the possibility of obtaining chance correlations. The optimal number of components (latent variables) was chosen on the basis of the highest cross-validated r^2 value and the smallest standard deviation. A 2 kcal/mol energy column filter was performed to improve the signal-to-noise ratio. The steric and electrostatic field columns were then used according to the COMFA STD default option.

From the above procedure, the final PLS Eq. (1) in Table 3 was derived as shown below.

$$pIC_{50}=2.423+0.872\times cLog\,P+[electrostatic]+[steric]$$

$$n=43,\ F(5,37)=170,\quad s=0.191,\quad r^2=0.958$$

The cLog P contribution in the equations in Table 3 and 4 is relatively high (18.4—21.4%). This suggests the compounds may penetrate the cell wall or interact strongly at the hydrophobic regions for showing the biological activity. The alignment produced good cross-validated results and conventional values with the optimum number of components. In this model, steric, electrostatic, and hydrophobic factors contributed to the QSAR equation by 40%, 41.3%, and 18.7%, respectively. It can be seen in Table 1 that the activity of all the examined compounds is calculated with an average absolute error of 0.14 log units. Figure 1 shows a plot of calculated *vs.* measured activities of stilbenes. A contour map of the coefficients of each grid point is depicted in Figs. 2 and 3.

CoMFA Results

The CoMFA statistical results for the cytotoxic activity of A549 are summarized in Table 3. In these equations, *m* indicates the number of optimum components and *s* is the standard deviation obtained from the leave-one-out cross-validation. The relative contribution of steric, electrostatic, and cLog P values is shown as a percentage. To determine whether the hydrophobic parameter is significant, cLog P values were inserted in the CoMFA analyses. As a result, their contribution to the equation was relatively high (18.4 to

21.4%) in most cases. We initially analyzed 43 compounds and obtained Eqs. (1)—(5). Among these equations, Eq. (1), which was derived from the overlapping of the compounds on conformer 1 as for a template structure, was the most significant. On the other hand, Eqs. (4) and (5) were obtained from conformers 8 and 12, respectively, which gave poor statistical results. We assumed that conformer 1 is the active form showing cytotoxicity. As depicted in Table 2, conformer 1 has 41.6° (τ1) and 47.3° (τ2) torsion angles. The calculated pIC_{50} values in Table 1 were derived from Eq. 1.

Table 2. Torsion Angle and Energy of Lead Template **1p**

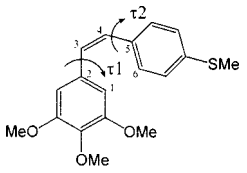

1p

No. of conformer	τ1	τ2	Energy (kcal/mol)	Minimized energy[a] (kcal/mol)
1	−150	−120	17.70	16.845[b]
2	150	150	17.73	15.940[c]
3	30	−120	17.74	16.717[d]
4	150	−60	17.80	16.940
5	60	−150	17.95	16.717
6	30	60	17.96	16.926
7	30	−150	18.03	16.717
8	60	30	18.05	16.782[e]
9	30	30	18.19	16.926
10	60	60	18.27	16.782
11	−120	−120	18.27	16.845
12	60	−120	18.34	16.750[f]
13	120	−60	18.42	16.940
14	−150	−150	18.45	16.845
15	−60	−60	18.47	16.880
16	−120	−150	18.47	16.845
17	−150	30	18.63	17.560
18	−150	60	18.63	17.560
19	−60	150	18.65	17.480
20	−120	30	18.70	17.560

Torsional angles in degree are defined with notations as follows: τ1: C1-C2-C3-C4, τ2: C3-C4-C5-C6. *a*) Energy minimized by the Tripos force field using the Gasteiger-Huckel charge. *b*) τ1: 41.6°, τ2: 47.3°; *c*) τ1: −43.8°, τ2: −44.1°; *d*) τ1: 40.4°, τ2: 42.2°; *e*) τ1: 44.1°, τ2: 44.2°; *f*) τ1: 43.6°, τ2: 42.2°.

Discussion

The application of CoMFA to a structurally varied set of 43 antitumor agents resulted in a reasonable 3-D QSAR model. Figures 2 and 3 represent the major steric and electrostatic potential contour maps drawn according to Eq. (1) in Table 3, respectively. The green zone is more important and located around the A and B rings of the stilbene derivatives according to the higher activity of the molecules. That area indicates regions where submolecular bulk is well accommodated with an increase in cytotoxicity, whereas the yellow areas indicate regions where the submolecular bulk is unfa-

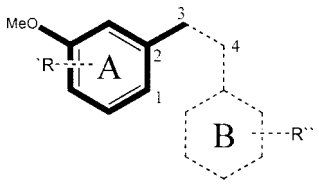

Chart 3. Template Molecules for Molecular Superposition

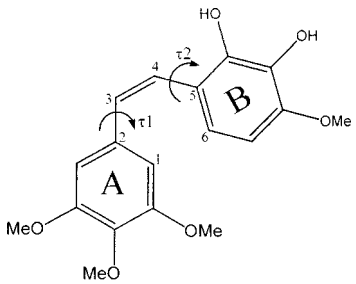

Chart 4. Structue of Combretastatin A-1. τ1: C1–C2–C3–C4, τ2; C3–C4–C5–C6, τ1: −58.1°, τ2: −15.7°

Table 3. CoMFA Correlation Statistics for Stilbenes (n=43)

Conformer	q^2	r^2	s	m	Contribution (%)			Equation	No.
					st.	el.	cLog P		
1	0.640	0.958	0.191	5	40.0	41.3	18.7	2.423+0.872×cLog P	1
2	0.632	0.921	0.260	4	33.3	45.3	21.4	2.557+0.828×cLog P	2
3	0.591	0.922	0.259	4	38.6	41.1	20.3	2.418+0.848×cLog P	3
8	0.527	0.928	0.249	4	42.3	39.3	18.4	2.627+0.800×cLog P	4
12	0.549	0.917	0.267	4	37.3	42.5	20.2	2.351+0.818×cLog P	5

Table 4. CoMFA Correlation Statistics Based on the X-Ray Structure of Combretastatin A-4 as a Lead Template

Alignment	q^2	r^2	s	m	Contribution (%)			Equation
					st.	el.	cLog P	
Reg	0.565	0.946	0.219	5	42.4	38.0	19.6	2.331+0.889×cLog P
Auto	0.513	0.913	0.274	4	37.6	43.9	18.4	2.676+0.769×cLog P

q^2: cross-validated R square, r^2: conventional R square, s: standard deviation, m: number of optimum components, st.: steric, el.: electrostatic, Reg: region defined manually to give the region as 16×18×14 Å (X=−11 to 5, Y=−7 to 11, Z=−10 to 4), Auto: region defined automatically to give the region as 19×22×22 Å (X=−14 to 5, Y=−10 to 12, Z=−12 to 10).

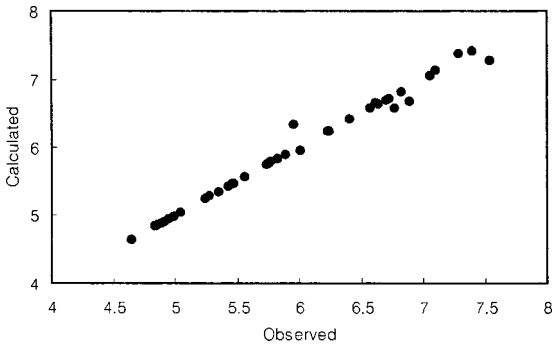

Fig. 1. Plot of the Calculated *versus* Observed pIC_{50} for the CoMFA Analysis of the 43 Compounds Aligned According to Eq. (1) in Table 4

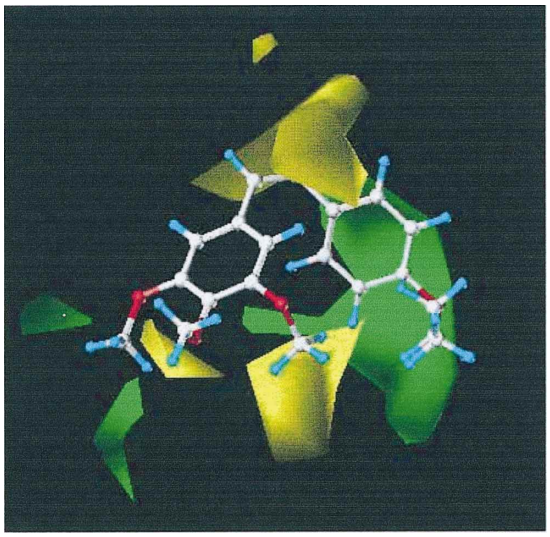

Fig. 2. Steric Contour Map from the CoMFA Mode for Combretastatins
Favoring activity: green, bulky group; yellow, less bulky group.

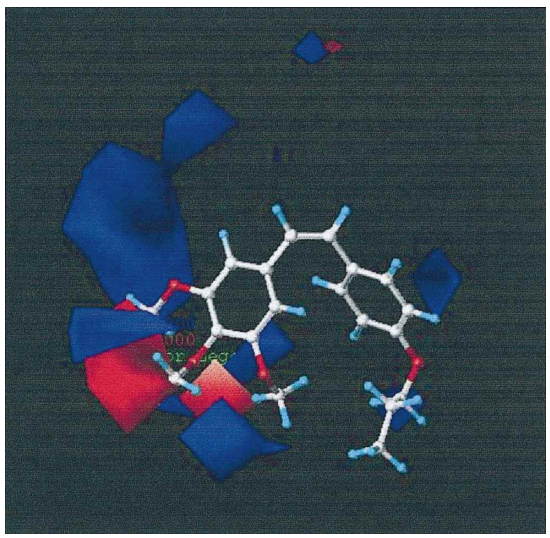

Fig. 3. Electrostatic Contour Map from the CoMFA Mode for Combretastatins
Favoring activity: blue, positive charge; red, negative charge group.

vorable for activity to occur. As can be seen in Fig. 2, it is well explained that bulky substitution at the *para*-position of ring B such as OPr, Br, Cl, and OMe groups contributes to the increase in activity. Therefore green polyhedra running parallel, mostly on the ring B side of the most active compounds such as **1a**, **1b**, **1f**, and **3c**, could also indicate favorable steric interactions of these structural elements with a large hydrophobic pocket at the active site. Small green contour regions, indicating favorable steric interactions with a possible *para*-substituent of the A ring located here are shown in the lower left corner of Fig. 2.

On the other hand, yellow contour regions that extend roughly perpendicular to the previously described green region accommodate the heteroaromatic ring position instead of ring B, which is the same as in *trans*-configuration compounds. A small steric yellow region of the upper area of the double bond external to the green region also suggests that the dimensions of these substituents cannot be too large or it will render the compound inactive (*i.e.*, **3e**). This corresponds to the spatial positions that do not contain heteroaromatic compounds such as **1l**—**o**, **2l**, and **3f**.

The red area indicates regions where the more negative electrostatic interaction with the receptor increases the activity, whereas the blue areas show regions where the reverse is the case. In a contour map, a positive electrostatic-potential region favoring activity appears on rings A and B. Its region is located in the outer zone of the trimethoxy group on ring A, whereas a negative electrostatic region favorable to activity is located at the oxygen atoms of trimethoxy groups on ring A. Compound **8** with a carboxyl group on the double bond is less active because the electronegative function is extended away from the favored region of interaction. Compounds that have heteroaromatic rings such as **1l**, **1m**, **1n**, and **3f** are less active because the rings contain electron-rich atoms that seem to not contribute to increased activity and are extended away from the favored region of interaction. According to this binding hypothesis, red polyhedra, indicating areas where high electron density within the ligands enhances affinity, overlap the aromatic electron density of the most active compounds. In compounds **1a**, **1b**, **1f**, and **3c**, with respect to the trimethoxy moiety, a red electrostatic contour and a green steric contour are present. Both of these regions express the preference of the trimethoxy group over the dimethoxy group at the active site. The most active compounds could also indicate favorable steric interactions of these structural elements with a large hydrophobic pocket at the active site. The descriptive characteristics of the present model are good and the plot of the calculated versus the observed pIC_{50} for the CoMFA of the 43 compounds is shown in Fig. 1. The reliability of a QSAR model is usually evaluated by testing its ability to predict the biological activity of newly designed molecules acting on the same biological system. In this study, the CoMFA model not only showed that the cytotoxicities of the 43 combretastatin derivatives had an excellent correlation with the electrostatic and steric field, but also provided an important pharmacophore model that could be useful in depicting the receptor sites three-dimensionally.

Acknowledgment This work was supported by a research grant from the Ministry of Health and Welfare of Korea (00-PJ1-PG1-CH15-0002).

References

1) Pettit G. R., Singh S. B., Hamel E., Lin C. M., Alberts D. S., Garcia-Kendal D., *Experientia*, **45**, 209—211 (1989).

2) Bai R., Pettit G. R., Hamel E., *Biochem. Pharmacol.*, **39**, 1941—1949 (1990).
3) Ferrigni N. R., McLaughlin J. L., Powell R. G., Smith C. R., *J. Nat. Prod.*, **47**, 347—352 (1984).
4) Gill M. T., Bajaj R., Chang C. J., Nichols D. E., McLaughlin J. L., *J. Nat. Prod.*, **50**, 36—40 (1987).
5) Lin C. M., Singh S. B., Chu P. S., Dempcy R. O., Schmidt J. M., Pettit G. R., Hamel E., *Mol. Pharmacol.*, **34**, 200—208 (1988).
6) McGown A. T., Fox B. W., *Cancer Chemother. Pharmacol.*, **26**, 79—81 (1990).
7) Jordan A., Hadfield J. A., Lawrence N. J., McGown A. T., *Med. Res. Rev.*, **18**, 259—296 (1998).
8) Ter Haar E., Rosenkranz H. S., Hamel E., Day B. W., *Bioorg. Med. Chem.*, **4**, 1659—1671 (1996).
9) Nandy P., Banerjee S., Gao H., Hui M. B., Lien E., *J. Pharmaceutical. Res.*, **8**, 776—781 (1991).
10) Brown M. L., Rieger J. M., Macdonald T. L., *Bioorg. Med. Chem.*, **8**, 1433—1441 (2000).
11) Kim S., Ko H., Park J. E., Jung S., Lee S. K., Chun Y.-J., *J. Med. Chem.*, **45**, 160—164 (2002).
12) Cramer R. D. III, Patterson D. E., Bunce J. D., *J. Am. Chem. Soc.*, **110**, 5959—5967 (1988).
13) Raghavan K., Buolamwini J. K., Fesen M. R., Pommier Y., Kohn K. W., Weinstein J. N., *J. Med. Chem.*, **38**, 890—897 (1995).
14) Rubinstein L. V., Shoemaker R. H., Paull K. D., Simon R. M., Tosini S., Skehan P., Scudiero D. A., Monks A., Boyd M. R., *J. Natl. Cancer Inst.*, **82**, 1113—1118 (1990).
15) Skehan P., Storeng R., Scudiero D., Monks A., McMahon J., Vistica D., Warren J. T., Bokesch H., Kenney S., Boyd M. R., *J. Natl. Cancer Inst.*, **82**, 1107—1112 (1990).
16) Alley M. C., Scudiero D. A., Monks A., Hursey M. L., Czerwinski M. J., Fine D. L., Abbott B. J., Mayo J. G., Shoemaker R. H., Boyd M. R., *Cancer Res.*, **48**, 589—601 (1988).
17) Mossman T., *J. Immunol. Meth.*, **65**, 55—63 (1983).
18) Wu F. Y. H., Liao W. C., Chang H. M., *Life Sci.*, **52**, 1797—1804 (1993).
19) The Sybyl program (Version 6.3) was supplied by Tripos Associates, 1699 South Hanley Road, Suite 303, St. Louis, Missouri 63144, U.S.A.
20) Pettit G. R., Singh S. B., Niven M. L., Hamel E., Schmidt J. M., *J. Nat. Prod.*, **50**, 119—131 (1987).
21) Cushman M., Nagarathnam D., Gopal D., He H.-M., Lin C. M., Hamel E., *J. Med. Chem.*, **35**, 2293—2306 (1992).
22) Cushman M., Nagarathnam D., Gopal D., Chakraborti A. K., Lin C. M., Hamel E., *J. Med. Chem.*, **34**, 2579—2588 (1991).